Antiviral Research 97 (2013) 232–239

Contents lists available at SciVerse ScienceDirect

Antiviral Research

journal homepage: www.elsevier.com/locate/antiviral

Selective inhibition of the West Nile virus methyltransferase by nucleoside analogs

Hui Chen [a], Lihui Liu [a], Susan A. Jones [a], Nilesh Banavali [a,b], Jorden Kass [c], Zhong Li [a], Jing Zhang [a], Laura D. Kramer [a,b], Arun K. Ghosh [c], Hongmin Li [a,b,*]

[a] Wadsworth Center, New York State Department of Health, 120 New Scotland Ave., Albany, NY 12208, USA
[b] Department of Biomedical Sciences, School of Public Health, State University of New York, Albany, P.O. Box 509, NY 12201, USA
[c] Department of Chemistry and Medicinal Chemistry, Purdue University, 560 Oval Drive, West Lafayette, IN 47907, USA

ARTICLE INFO

Article history:
Received 18 May 2012
Revised 14 December 2012
Accepted 15 December 2012
Available online 22 December 2012

Keywords:
Flavivirus NS5
RNA cap methylation
West Nile virus
Methyltransferase
Antiviral development

ABSTRACT

The flavivirus methyltransferase (MTase) sequentially methylates the N-7 and 2′-O positions of the viral RNA cap (GpppA-RNA→m^7GpppA-RNA→m^7GpppAm-RNA), using S-adenosyl-L-methionine (SAM) as a methyl donor. We report here the synthesis and biological evaluation of a series of novel nucleoside analogs. Two of these compounds can effectively and competitively inhibit the WNV MTase with IC_{50} values in micromolar range and, more importantly, do not inhibit human MTase. The compounds can also suppress the WNV replication in cell culture.

1. Introduction

Most flaviviruses, such as dengue viruses (DENVs), West Nile virus (WNV), yellow fever virus (YFV), Japanese encephalitis virus (JEV), and tick-borne encephalitis virus (TBEV), cause significant human disease. Approximately 2.5 billion people are at risk of DENV infection, with an estimated 500,000 cases of life-threatening disease per year. In addition, WNV is now the leading cause of arboviral encephalitis in the US (USGS, 2010), resulting in more than a thousand human deaths (CDC, 2010). However, vaccines for humans currently are available only for YFV, JEV, and TBEV (Burke and Monath, 2001); and more importantly no clinically approved antiviral therapy is available for treatment of flavivirus infection. Therefore, it is a public health priority to develop antiviral agents for post-infection treatment (Kramer et al., 2007; Sampath and Padmanabhan, 2009).

Most eukaryotic and viral mRNAs possess a 5′-cap that is important for mRNA stability and efficient translation (Furuichi and Shatkin, 2000). We and others have shown that recombinant NS5 proteins from various flaviviruses possess both N-7 and 2′-O MTase activities (Dong et al., 2007; Egloff et al., 2002; Kroschewski et al., 2008; Ray et al., 2006; Zhou et al., 2007). Flavivirus MTase has been shown to be essential for WNV (Dong et al., 2007; Zhou et al., 2007), KUNV (Khromykh et al., 1998), YFV (Bhattacharya et al., 2008), and DENV replication (Kroschewski et al., 2008). Several MTase inhibitors, some of which showed antiviral efficacy in cell cultures, have been reported (Benarroch et al., 2004; Dong et al., 2008b; Lim et al., 2008, 2011; Luzhkov et al., 2007; Milani et al., 2009; Podvinec et al., 2010; Selisko et al., 2010). Some of these potential inhibitors targeted the co-factor SAM-binding site. However, it was known that SAM is also a methyl donor for host RNA and protein methylations. Inhibitors targeting the SAM pocket may nonspecifically suppress host MTases, resulting in toxicity. We have identified a flavivirus-specific pocket near the SAM-binding site of flavivirus MTase (Dong et al., 2010). Recently, a highly selective inhibitor of the flavivirus MTase but not against human MTases was reported to target this pocket, although the antiviral efficacy of the compound has not been characterized (Lim et al., 2011).

The aim of the present study was to investigate whether selective inhibitors can be identified. We chose five nucleoside analogs and found that these nucleoside analogs can inhibit the methyltransferase activities of the WNV MTase to various degrees. Two compounds were found to have higher potency than others and they did not inhibit the activity of human RNA MTase.

* Corresponding author at: Wadsworth Center, New York State Department of Health, 120 New Scotland Ave., Albany, NY 12208, USA. Tel.: +1 518 486 9154; fax: +1 518 408 2190.
E-mail address: lih@wadsworth.org (H. Li).

0166-3542/$ - see front matter © 2012 Elsevier B.V. All rights reserved.
http://dx.doi.org/10.1016/j.antiviral.2012.12.012

2. Materials and methods

2.1. Compounds

The nucleoside analogs were synthesized as previously described (Ghosh and Kass, 2010). Sinefungin (SIN) was purchased from Sigma–Aldrich. S-adenosyl-methionine (SAM) was purchased from New England Biolabs. [α-^{32}P]GTP was purchased from MP Biomedicals.

2.2. In vitro MTase inhibition assay

The 5′-end-labeled substrates G*pppA-RNA and m^{7}G*pppA-RNA, representing the first 90 nucleotides of the WNV genome (the asterisk indicates that the following phosphate is ^{32}P labeled), were prepared as described previously (Dong et al., 2008b; Zhou et al., 2007). The N-7 and 2′-O methylation inhibition assays were performed as described previously (Dong et al., 2008b; Ray et al., 2006). The N-7 methylation was measured by conversion of G*pppA-RNA→m^{7}G*pppA-RNA. The 2′-O methylation was monitored by conversion of m^{7}G*pppA-RNA→m^{7}G*pppAm-RNA. Both methylation assays were performed with 1.5 μM WNV MTase, 80 μM SAM, 0.36 μM G*pppA-RNA or m^{7}G*pppA-RNA substrate, and various concentrations of each compound. The methylation reactions were digested with nuclease P1 to release cap moieties (m^{7}G*pppAm, m^{7}G*pppA, and G*pppA). The cap molecules were separated on a thin-layer chromatograph (TLC), and quantified by a PhosphorImager (Dong et al., 2008b; Ray et al., 2006). The percentage of activity was determined after quantification of m^{7}G*pppA, m^{7}G*pppAm, and G*pppA. The IC_{50} value, unless specified, was determined by fitting of the dose–response curve using the ORIGIN software package. K_i was calculated according to the Cheng–Prusoff equation (Cheng and Prusoff, 1973) ($K_i = IC_{50}/(1 + [S]/K_m)$, where K_i is the inhibition constant of the inhibitor, [S] is substrate concentration and K_m is the concentration of substrate at which enzyme activity is at half maximal (Chung et al., 2010)).

2.3. Inhibition of human RNA MTase (hRNMTase)

The human guanine N-7 RNA MTase was overexpressed as a GST-fusion protein in *Escherichia coli*. BL21 (DE3) cells as previously described (Pillutla et al., 1998). Recombinant hRNMTase was purified through a glutathione Sepharose 4B affinity column (GE Healthcare), followed by gel filtration chromatography using a Superdex S-200 column (GE Healthcare) to ensure that protein purity was >99%. The protein was concentrated using an Amicon stirred cell (Millipore), aliquoted and stored at −80 °C.

The inhibition assay of hRNMTase was performed with the same condition used for the WNV N-7 MTase inhibition assay, except that the WNV MTase was replaced by hRNMTase. The hRNMTase reaction contained 0.3 μM hRNMTase, 80 μM SAM, 0.36 μM 5′-end-labeled 90nt WNV substrates G*pppA-RNA, and compounds at various concentrations.

2.4. SAM binding assay

A G25 filtration assay was used to evaluate compound competitive inhibition of SAM binding to the WNV MTase. A 50-μl reaction mixture contains 0.6 μM WNV MTase (or 0.12 μM hRNMTase), 1 μl of 10-fold diluted [methyl-^{3}H]-SAM (78 Ci/mmol, Perkin Elmer) (about 14.1 nM final concentration), and each compound at a concentration series of 3-fold dilution of 60 μM (or 300 μM for hRNMTase). The reaction mixtures were incubated at room temperature for 2 h, loaded to the Biomax Spin-25 Mini-column, and centrifuged at 5000 rpm for three minutes. Eluted samples were quantified by Geiger scintillation counter (Beckman LS6500). All data points were done in duplicate.

2.5. Ligand docking

The initial 3D coordinates for compound 2 were generated using the Frog2.1 server (http://bioserv.rpbs.jussieu.fr/cgi-bin/Frog2) (Miteva et al., 2010) from the SMILES description for compound 2, with no additional optimization. The parameters used were: no disambiguation, no stage 2 Monte-Carlo, no minimization, a single conformation requested, Ewindow 50.0, Emax 500.0, and RMSD 0.8. CHARMM General Force Field (CGENFF) topology and parameters (Vanommeslaeghe et al., 2010) for the compound were then generated using the ParamChem server (https://www.paramchem.org/) (Malde et al., 2011), with the parameters for the silicon atom obtained by transfer of parameters from an alkyl tetrahedral carbon. All further optimization and docking of the compound were performed using the CHARMM program, version 35b3 (Brooks et al., 2009). The initial compound conformation was optimized using 10,000 steps of steepest descent (SD) and adopted basis Newton Raphson (ABNR) minimizations with a harmonic constraint of 0.5 kcal/mol on all non-hydrogen atoms and a convergence tolerance of 0.0001 kcal/mol between successive steps. The compound was then oriented in the binding pocket of the WNV MTase using corresponding non-hydrogen atoms of the furanose sugar entity in the inhibitor sinefungin (PDB ID: 3LKZ, chain A). The sugar atoms used in the orientation were then fixed and the rest of the compound was optimized in isolation using optimization protocol 1, which consisted of (a) 10,000 SD and ABNR steps with a tolerance of 0.01 kcal/mol, (b) 2000 steps of Langevin dynamics at 1000 K with a friction coefficient of 1.0/ps, (c) 10,000 SD and ABNR steps with a tolerance of 0.01 kcal/mol. The compound was then optimized further in the presence of the protein by simulated annealing, first with its sugar non-hydrogen atoms and all protein atoms held fixed, then with the same sugar atoms and all non-hydrogen atoms of the protein held by weak harmonic constraints of 1 kcal/mol. The simulated annealing consisted of successive application of protocol 1 with a temperature bath for the Langevin dynamics set to 100, 200, 300, 200, and 100 K. It was observed that the sidechain of His110 reoriented significantly from the original crystal structure due to steric clashes with the 2′ sugar substituent in compound 2. The interaction of this sidechain was further optimized in isolation using protocol 1 and additional miscellaneous mean field potential (MMFP) distance restraints between atoms ND1 and NE2 of His110 and the nearest oxygen atom of compound 2. The vacuum interaction energy between compound 2 and the WNV MTase in this final docked conformation was −97.8 kcal/mol, which decomposed into a van der Waals component of −58.6 kcal/mol and an electrostatic component of −39.2 kcal/mol.

2.6. Cytotoxicity assay

Cytotoxicity was measured by a MTT cell proliferation assay using the 3-(4,5-dimethylthiazol-2-yl)-2,5-diphenyl tetrazolium bromide method(ATCC). Approximately 2×10^4 human A549 cells in 100 μl of media were seeded into 60 wells of a 96 well plate, the remaining wells held media. Plates were held at RT for 1 h and then incubated for 20–24 h. The media was removed and 100 μl of media containing decreasing concentrations of antiviral compound in 1% DMSO were added to the wells. All determinations were performed in triplicate. After 42 h incubation at 37 °C, 10 μl of MTT was added to the wells and incubated another 3 h. Detergent (100 μl) was placed in the wells and the plate was incubated for 3 h at room temperature in the dark. A microtiter plate reader (Ely808, BioTek Instruments, Inc.) with a 570 nm filter was used

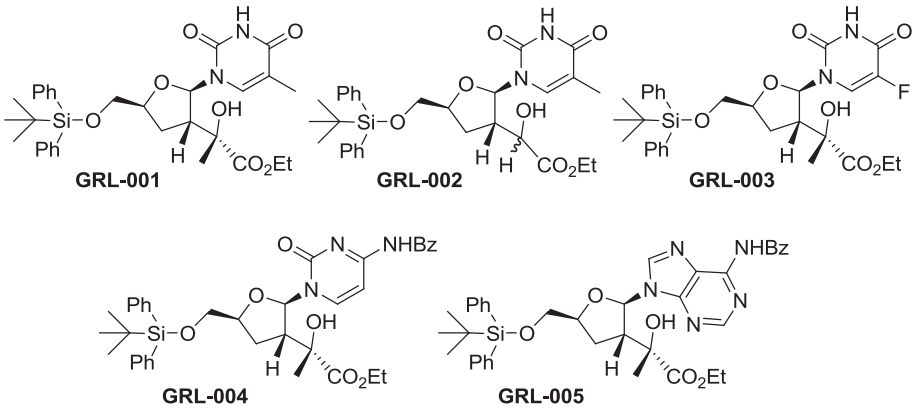

Fig. 1. Chemical structures for the 5 WNV MTase inhibitor nucleoside analog compounds synthesized, named GRL-001 to GRL-005.

to record absorbance. All determinations were performed in triplicate. After adjusting the absorbance for background and comparing to untreated controls, a dose–response curve was plotted using GraphPad Prism software, (GraphPad Software, La Joll, CA, USA). The cytotoxic concentration CC_{50} (the concentration of inhibitor required to reduce cell viability by 50%) was calculated using nonlinear regression to fit the dose–response curve using the ORIGIN software package.

2.7. Antiviral assay

A viral titer reduction assay was used to determine the compounds effect on WNV. Approximately 2×10^5 human A549 cells in 500 μl of media were seeded into each well of a 24 well plate. At 24–30 h after seeding, dilutions at 2× the desired concentration of the compound were made in 2% DMSO media and 250 μl was added to wells in triplicate. Immediately following, 250 μl of media containing WNV (NY99) at a concentration to yield a MOI 0.1 PFU/cell, was added to the wells. After 42 h incubation at 37 °C, culture media was collected, and stored at −80 °C for later quantification using a plaque assay. For the plaque assay, Vero cell monolayers in 6-well plates were seeded 3–4 days prior to infection to achieve a confluent monolayer. Depending on the virus, three to eight 10-fold serial dilutions of the harvested samples were made, three to five dilutions of the virus were tested. To inoculate, 100 μl of the dilution is inoculated into each of two wells, rocked gently to distribute virus, and incubated for 1 h at 37 °C. Cells are then overlaid with a nutrient medium containing 0.6% oxoid agar. The agar is

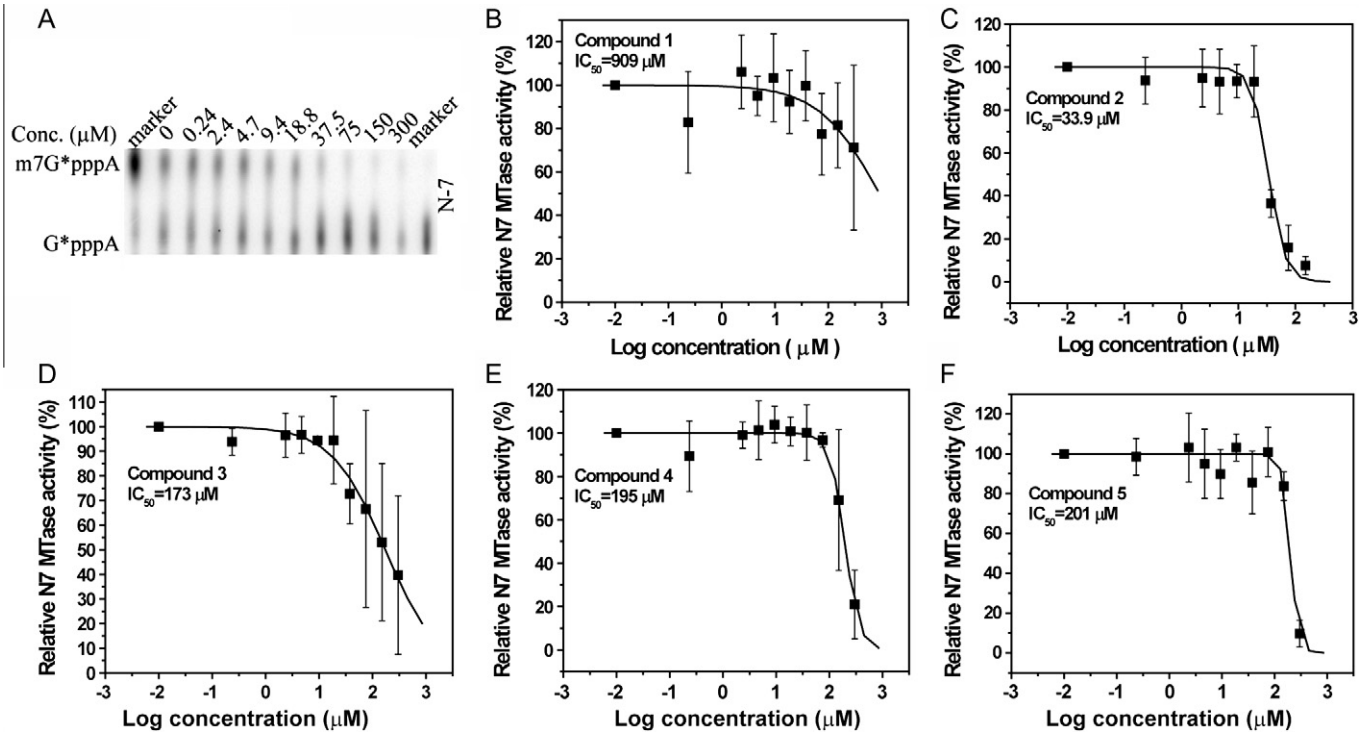

Fig. 2. Inhibition of the N-7 methylation activity of the WNV MTase by nucleoside analogs. (A) Inhibition of the N-7 methylation activity of the WNV MTase by GRL-002 was analyzed on TLC plates. The N-7 methylation was measured by conversion of G*pppA-RNA→m^{7}G*pppA-RNA (the asterisk indicates that the following phosphate is ^{32}P labeled; the RNA represents the first 90 nucleotides of the WNV genome). The spots representing different cap structures on TLC plates were quantified by a PhosphorImager. The methylation activity without GRL-002 was set at 100%. The migration positions of the G*pppA and m^{7}G*pppA molecules are labeled on the side of the TLC images. (B–F) Curve fitting to determine the IC_{50} values for each compound on the N-7 MTase activity of the WNV MTase. The percentage of activity was determined after quantification of G*pppA and m^{7}G*pppA. The IC_{50} value was determined by fitting of the dose–response curve as described in methods section. Each reaction was carried out in triplicate and the standard deviation is plotted.

allowed to solidify and the plates are then incubated at 37 °C. A second overlay containing 2% neutral red is added after the plaques begin to appear on day 2, and then incubated overnight. Plaques are counted daily for 1–3 days until no significant increase is seen. The effective concentration EC_{50} (the concentration of inhibitor required to reduce virus growth by 50%) was determined by nonlinear regression fitting of the dose–response curve using the ORIGIN software package.

3. Results

3.1. Nucleoside analogs showed inhibition of flavivirus MTase

In order to identify new specific inhibitors against flavivirus MTase, we chose five nucleoside analogs to investigate the effects of these analogs on the MTase activities (Fig. 1). These analogs were chosen rationally, based upon the inhibitor sinefungin-bound MTase structure (Dong et al., 2010). Our preliminary docking studies indicated that the synthetic nucleosides can bind well in the substrate-binding site. Compound GRL-001 is the prototypical compound containing a thymine base on the tetrahydrofuran backbone. It also contains a quaternary center also present in compounds GRL-003, GRL-004, and GRL-005. All five compounds contain a hydrophobic methyl *tert*-butyl diphenyl silyl ether. Compound GRL-002 removes the methyl group from the quaternary center probing its importance. Compound GRL-003 substitutes fluorouracil for thymine as the nucleobase. Fluorouracil derivatives are known to have activity against various strains of cancer and are used clinically (Longley et al., 2003). Compound GRL-004 contains benzoyl cytosine as the nucleobase. Compounds GRL-001 through GLR-004 all contain pyrimidines as the nucleobase. Compound GRL-005 contains a benzoyl adenine as the nucleobase as an example of a purine base.

We used the WNV MTase as a model MTase. Our results indicated that compounds 1, 4, and 5 only inhibited the N-7 and 2′-O MTase activities at very high concentration (Figs. 2 and 3, Table 1). In contrast, GRL-002 efficiently inhibited the N-7 MTase activity of the WNV MTase with a K_i of 24.2 μM, and inhibited the 2′-O MTase activity with a K_i of 3.9 μM. In addition, although compound 3 only moderately inhibited the N-7 MTase activity, it inhibited the 2′-O MTase activity of the WNV MTase with a K_i of 14.1 μM.

In addition, we noticed that some of the dose response curves showed Hill coefficients larger than 1, particularly for the 2′-O MTase inhibitions. The high Hill coefficients may indicate that there are more than one binding sites on the WNV MTase for these nucleoside analogs, as suggested by a number of studies (Prinz, 2010; Shoichet, 2006). The results are consistent with the existence of an additional GTP-binding site for flavivirus MTase (Benarroch et al., 2004; Egloff et al., 2002; Zhou et al., 2007). Nucleoside analog ribavirin and a number of cap analogs have been shown to bind to this GTP binding site (Assenberg et al., 2007; Benarroch et al., 2004; Egloff et al., 2007; Geiss et al., 2009; Yap et al., 2010). Since the compounds used here are nucleoside analogs, they are expected to bind to the GTP-binding site in addition to the SAM binding site. Therefore, a high Hill coefficient is expected. Moreover, our results are also consistent with results from functional studies, which indicated that mutations within the GTP-binding site only affected the 2′-O but not the N-7 MTase activity (Dong

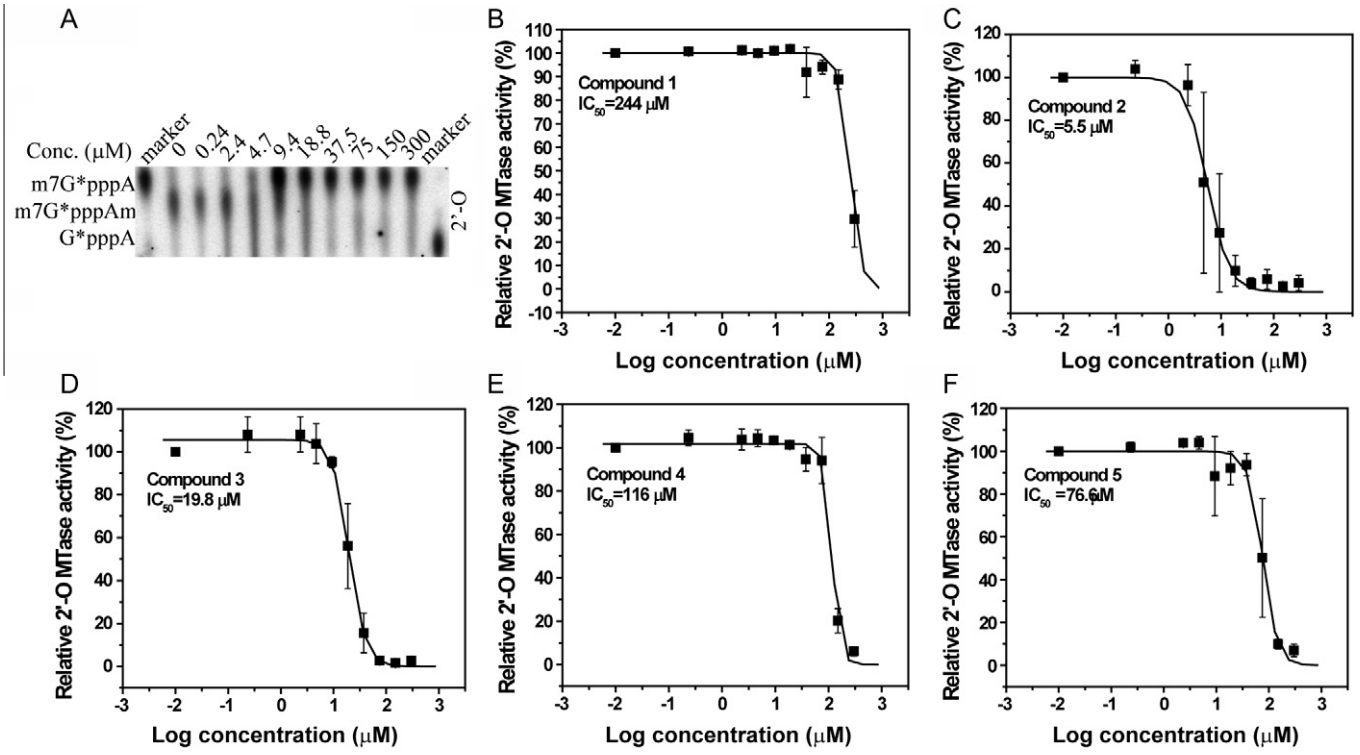

Fig. 3. Inhibition of the 2′-O methylation activity of the WNV MTase by nucleoside analogs. (A) Inhibition of the 2′-O methylation activity of the WNV MTase by compound 2 was analyzed on TLC plates. The 2′-O methylation was measured by conversion of m^7G^*pppA-RNA→m^7G^*pppAm-RNA (the asterisk indicates that the following phosphate is ^{32}P labeled; the RNA represents the first 90 nucleotides of the WNV genome). The spots representing different cap structures on TLC plates were quantified by a PhosphorImager. The methylation activity without compound 2 was set at 100%. The migration positions of the G^*pppA, m^7G^*pppA, and m^7G^*pppAm molecules are labeled on the side of the TLC images. (B–F) Determination of the IC_{50} values for each compound on the 2′-O MTase activity of the WNV MTase. The percentage of activity was determined after quantification of m^7G^*pppA and m^7G^*pppAm. The IC_{50} value was determined by fitting of the dose–response curve as described in methods section. Ki was calculated according to the Cheng-Prusoff equation (Cheng and Prusoff, 1973) ($K_i = IC_{50}/(1+[S]/K_m)$, where K_i is the inhibition constant of the inhibitor, [S] is substrate concentration and K_m is the concentration of substrate at which enzyme activity is at half maximal). Each reaction was carried out in triplicate and the standard deviation is plotted.

Table 1
Ki values of compound against the WNV MTase.

Compound	K_i (N-7) (μM)	Hill coefficient	K_i (2′-O) (μM)	Hill coefficient
1	649	0.8	174	4.1
2	24.2	3.0	3.9	2.1
3	123	0.9	14.1	2.8
4	139	3.2	82.8	5.4
5	143	5.6	54.7	3.2

et al., 2008a). Binding of these nucleoside analogs to the GTP-binding site of the MTase would result in additional inhibition of the 2′-O MTase activity, whereas the N-7 MTase activity would be largely unaffected. Consistently, our inhibition data indicated that the 2′-O MTase activity was inhibited more efficiently by these compounds than was the N-7 MTase activity (Table 1). Similar observations have been reported in another study (Lim et al., 2011).

3.2. Nucleoside analogs competitively inhibit SAM-binding to the WNV MTase

In order to determine whether these nucleoside analogs inhibit the methylation reactions through competitive binding to the SAM-binding site of the MTase, we examined the ability of the compounds to compete against ^{3}H-labeled SAM–MTase complex formation (Fig. 4). As a positive control, sinefungin (SIN) inhibited formation of the ^{3}H-labeled SAM–MTase complex very efficiently in a dose-dependent manner (Fig. 4A). Similarly, increasing amounts of GRL-002 and -003 led to decreasing amounts of ^{3}H–SAM–MTase complex formation (Fig. 4B and C). At 6.7 μM concentration, GRL-002 and -003 inhibited ^{3}H–SAM–MTase complex by 90% and 84%, respectively; and the ^{3}H–SAM–MTase complex was completely abolished by both compounds at 60 μM concentration. Our results indicated that both GRL-002 and -003 are competitive inhibitors.

3.3. Nucleoside analogs do not inhibit human RNA MTase

In order to determine whether the compounds can cross-inhibit human MTases, we expressed and purified human RNA guanine-7-MTase (hRNMTase), as described (Pillutla et al., 1998) (Fig. 5A). We first performed experiment to evaluate inhibition of hRNMTase by a known inhibitor, SIN, using a protocol modified from that described by Pillutla et al. (1998) (Fig. 5B). Since the hRNMTase does not have substrate specificity, we used the same capped G*pppA-RNA substrate as we used for analysis of inhibition of the WNV MTase to reduce systematic errors. As shown in Fig. 5B and C, the IC_{50} (compound concentration required for 50% inhibition of enzyme activity) value for SIN inhibition of hRNMTase is about 41.2 μM.

We next performed experiment to evaluate inhibition of hRNMTase by nucleoside analogs. As shown in Fig. 5C and D, compounds 2 and 3, which showed anti-viral MTase activity at micromolar concentrations (Figs. 2 and 3), did not inhibit the human hRNMTase activity even at 300 μM compound concentration. In consistent with results from the enzymatic activity experiment, [^{3}H] SAM competition binding assay showed that compounds 2 and 3 at 300 μM concentration did not inhibit [^{3}H] SAM binding to hRNMTase at all (Fig. 5E), whereas control SIN decreased the SAM binding very efficiently (Fig. 5F). These results indicated that compounds 2 and 3 specifically and competitively inhibited viral MTase but not human RNA MTase.

3.4. Analysis of the docking of GRL-002 into the crystal structure of the WNV MTase

To understand how GRL-002 inhibits the MTase, we docked the compound into its co-factor SAM-binding site. As shown in Fig. 6A, GRL-002 fits well in this pocket of the MTase. The docking of GRL-002 was performed using the orientation of sinefungin, a SAM analog inhibitor (Fig. 6B), as a guide. The thymine in GRL-002 is located in the same position as the adenine in sinefungin, and their sugar moieties also overlay well, as expected. There are potentially seven hydrogen bonds (H-bonds) between GRL-002 and the WNV MTase (Fig. 6B), a majority of which involve oxygen atoms in the sugar and thymine moieties of the compound. Sinefungin also binds to the WNV MTase with seven H-bonds, but these are distributed between its adenine (four H-bonds) and methionine (three H-bonds) moieties (Zhou et al., 2007). The total number of H-bonds being maintained may explain the similar inhibition activity between GRL-002 and sinefungin (Dong et al., 2008b). The methyl ter-butyl diphenyl silyl ether moiety of GRL-002, while differing significantly in bulkiness and polarity, fits into the same cleft as the corresponding methionine group of sinefungin. One of its phenyl rings is surrounded by E149, R213, E218, and Y220 sidechains of the MTase residues (Fig. 6B). The interactions between this moiety of GRL-002 and the MTase are mainly hydrophobic and these could be responsible for the selective inhibition of viral MTase over human MTase.

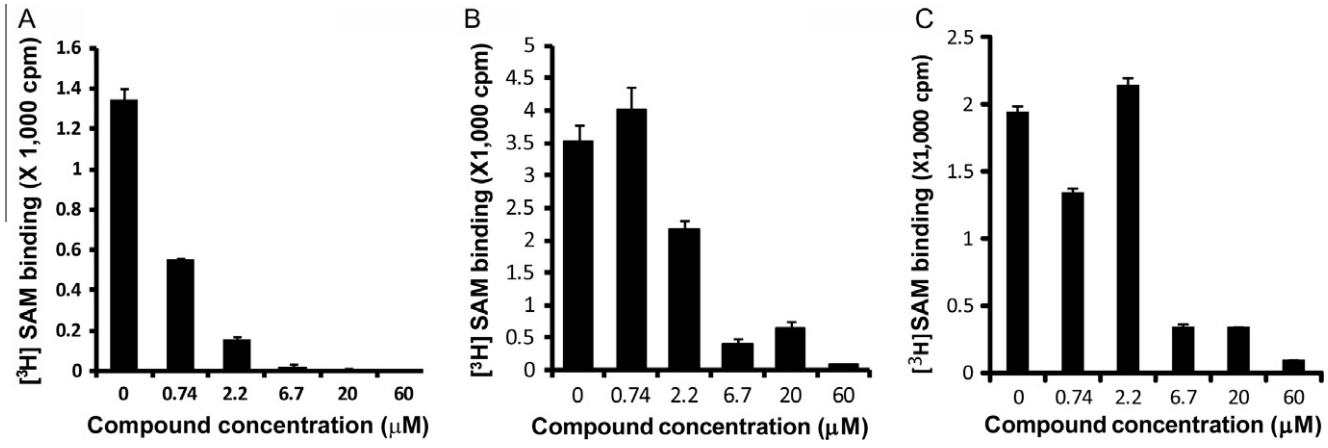

Fig. 4. [^{3}H] SAM competition assay. (A) Dose response of control SIN in inhibition of SAM-MTase complex formation. (B and C) Competitive binding of GRL-002 (A) and -003 (B) to abolish the SAM-MTase complex formation. WNV MTase and ^{3}H-labeled SAM were incubated with or without compounds SIN, GRL-002 and -003. A 3-fold dilution series was shown for each compound. The reaction mixtures were purified through Sephadex G-25 spin columns, and quantified by liquid scintillation counter.

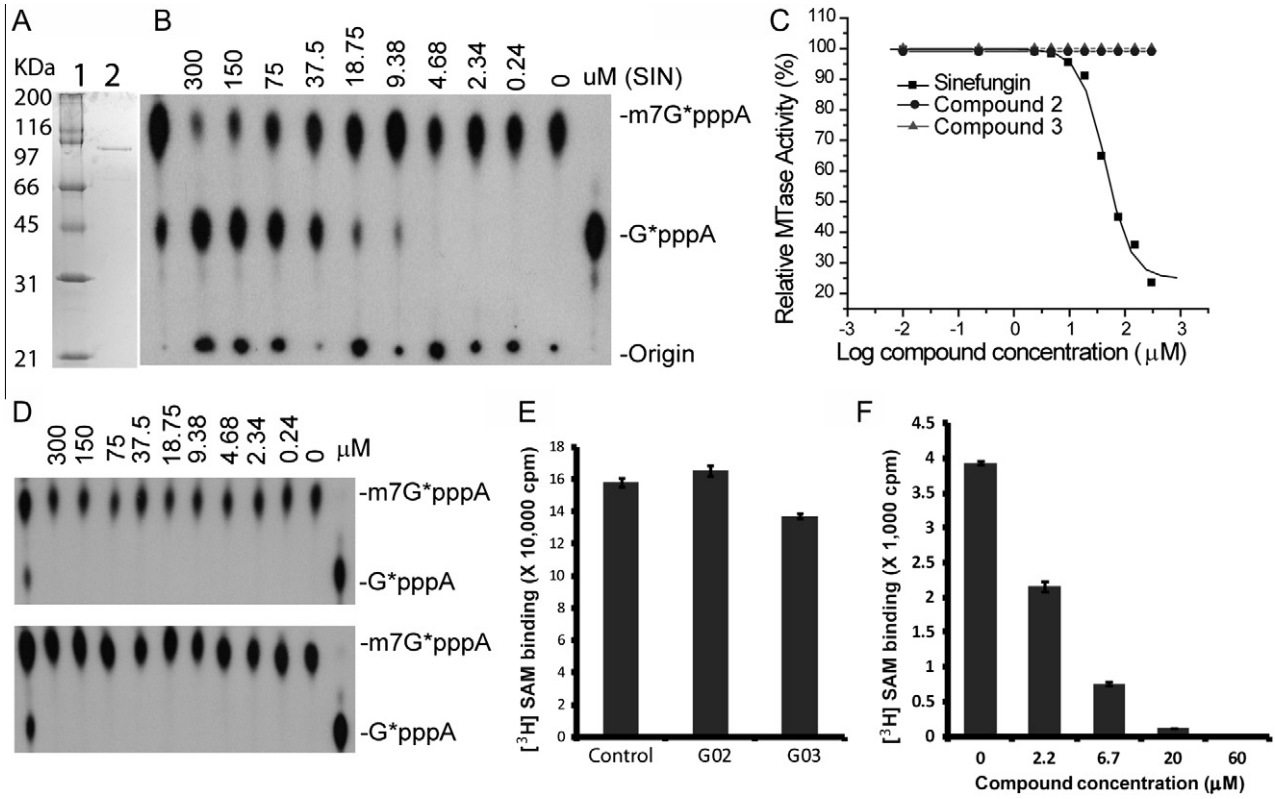

Fig. 5. Inhibition analysis of purified hRNMTase by sinefungin (SIN) and selected nucleoside analogs. (A) SDS–PAGE analysis of purified GST-hRNMTase fusion protein. A broad range molecular weight marker (Bio-Rad) was included in lane 1. (B) Inhibition of the hRNMTase activity by SIN analyzed on TLC plates. The methylation was measured by conversion of G*pppA-RNA to m^7G*pppA-RNA (the asterisk indicates that the following phosphate is ^{32}P labeled). Serial dilutions of SIN were indicated. Standard G*pppA (far right) and m^7G*pppA (left) were also included along each side of the plate. (C) Curve fitting to determine IC_{50} for inhibition of the hRNMTase by SIN (B), by compound 2 (D, upper panel) and by GRL-003 (D, lower panel). The methylation activity without inhibitors was set at 100%. (D) Inhibition of the hRNMTase activity by compound 2 (upper panel) and GRL-003 (lower panel), analyzed similarly as described in panel (B). Compound concentrations were marked. (E) Analysis of compounds GRL-002 and -003 at 300 μM concentration in inhibition of [^{3}H] SAM binding to human RNMTase. (F) Dose response of control SIN in inhibition of SAM–hRNMTase complex formation.

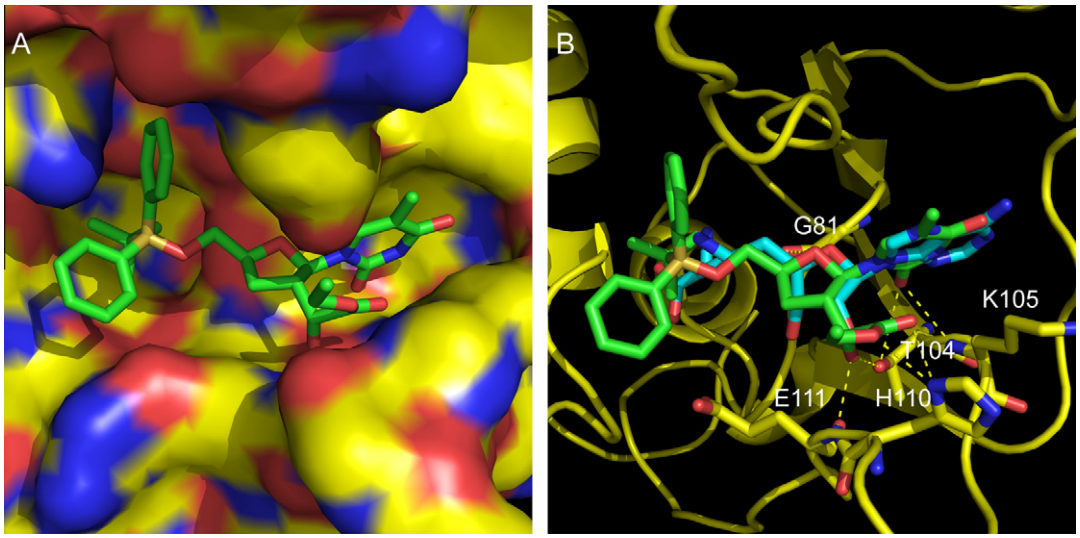

Fig. 6. GRL-002 and sinefungin binding to the SAM site of the WNV MTase. (A) Predicted structure of GRL-002 (stick representation) in the surrounding solvent-accessible surface of the MTase. Atomic color coding is as follows (unless otherwise specified): carbon in yellow/green, oxygen in red, nitrogen in blue, hydrogen in white, and silicon in orange. (B) Overlay of docked GRL002 and sinefungin in crystal structure (Dong et al., 2010). The MTase residues in polar contacts with GRL-002 are also shown in stick format. Color coding is the same as in (A), except sinefungin carbons are shown in cyan.

The observed differences in activities for all five compounds can be analyzed using the docked structure. GRL-001 itself has very low inhibitory activity towards the WNV MTase. Removing a methyl group and altering the stereochemistry of the chiral carbon attached to the 2′-position of the sugar may introduce an H-bond to Thr104, and leads to a dramatic enhancement in GRL-002, with K_i values 26 (N-7 inhibition) to 45 (2′-O inhibition) fold lower than those of GRL-001 (Table 1). A single CH3 to F modification in the thymine base in GRL-003 possibly introduces an H-bond with the E149 sidechain, and causes a 5 (N-7 inhibition) to 12

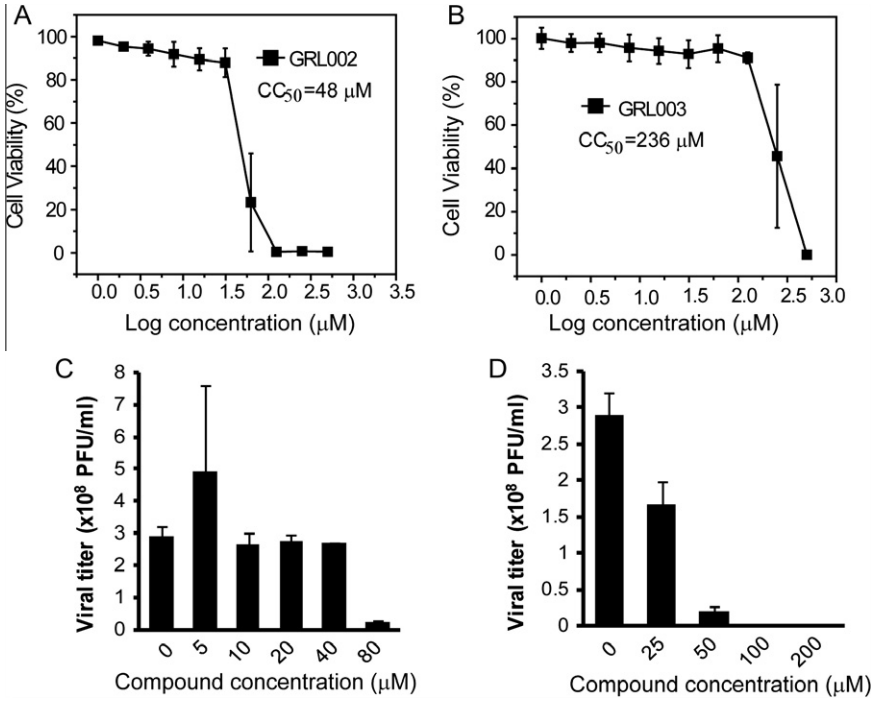

Fig. 7. Cytotoxicity and antiviral analyses for compounds 2 and 3. (A and B) Cytotoxicity of GRL-002 (A) and -003 (B). A549 cells were incubated with various concentrations of the compound and then assayed for viability at 42 h postincubation. (C and D) Inhibition of viral replication by GRL-002 (C) and -003 (D). A549 cells were infected with WNV at a multiplicity of infection of 0.1, in the presence or absence of SIN. At 42 h post-infection, viral titers in culture fluids were quantified by plaque assays on Vero cells.

(2′-O inhibition) fold enhancement. Compounds GRL-004 and -005 differ from GRL-001, -002, and -003 in the thymine group being replaced with benzyl cytosine and benzyl adenine, respectively, which could add hydrophobic interactions with F133 and nearby residues. This may explain a lesser, but still significant, 2–5-fold decrease in K_i values obtained by these base substitutions (Table 1), which also indicates that the base moiety could tolerate large structural changes.

3.5. Cytotoxicity and antiviral analyses

Upon confirming the anti-MTase activities of compounds 002 and 003, we performed cell-based assays to evaluate their biological activities. We first used a MTT cell proliferation assay to measure the cytotoxicity of these two compounds to a human A549 cell line (Fig. 7A and B). Our results indicated that compounds GRL-002 and -003 showed CC_{50} values of 48 and 236 μM respectively.

We next performed viral titer reduction assay to evaluate the compound antiviral efficacy. As shown in Fig. 7C and D, GRL-002 and -003 led to one logarithmic order of reduction in the WNV replication at 80 μM and 50 μM concentrations, respectively. The 50% effective concentrations (EC_{50}) of GRL-002 and -003 were estimated as 52 and 27 μM respectively.

4. Conclusions

Due to a lack of clinically approved therapeutic options, there is a great need for drugs that can specifically inhibit enzymes that are essential for the flavivirus life cycle. Previous studies have shown that N-7 methylation activity is essential for the WNV life cycle, therefore the viral MTase represents an attractive target for flavivirus therapy (Benarroch et al., 2004; Dong et al., 2010; Dong et al., 2008a,b; Lim et al., 2011; Liu et al., 2010; Ray et al., 2006; Zhou et al., 2007).

In this work, we sought to synthesize selective inhibitors against the WNV MTase. We identified two nucleoside analogs which are potent inhibitors of the WNV MTase, but do not inhibit human RNA MTase. In addition, one of the compounds, GRL-003, can also inhibit WNV growth in cell culture, with a good therapeutic window. Interestingly, although GRL-003 is less potent in inhibition of the MTase activities of the WNV MTase than GRL-002 *in vitro*, the GRL-003 can reduce virus growth in cell culture more robustly than the GRL-002. However, since the CC_{50} and EC_{50} of GRL-002 are very close, the antiviral effect of GRL-002 could not be distinguished from the cytotoxicity effect. Therefore the EC_{50} for GRL-002 might not reflect its true antiviral efficacy. In addition, inhibition data based on *in vitro* enzymatic assay may not be necessarily correlated with the data from cell-based assays, since in cell-based assay, the efficacy of a compound is affected not only by its ability to inhibit a particular target enzyme but also by a number of other factors such as compound permeability and drug metabolism (Copeland, 2005). It is possible GRL-003 is more permeable than GRL-002, resulting in a higher antiviral efficacy for GRL-003 than for -002. Alternatively, it is also possible that these nucleoside analogs act on other viral elements and/or host proteins. Nevertheless, selectivity of these analogs does not seem to be due to interactions with the pocket that binds the adenine moiety of the SAM cofactor, which was used to identify selective flaviviral MTase inhibitors previously (Dong et al., 2010; Lim et al., 2011). The selectivity of our unnatural nucleosides may be due to substituent groups introduced near the pocket that binds methionine moiety of the SAM co-factor. Further work to solve the structure of the MTase in complex with these inhibitors is necessary to gain insight into this selectivity. Our results suggest that inhibitor compounds could be made more selective through substitutions targeting two different clefts of the SAM-binding region of the flaviviral MTase.

Acknowledgements

This research was partially supported by grants (AI07079201A1 to H.L. and AI 09433501 to L.D.K., A.K.G. and H.L.) from the National

Institute of Health (NIH). The authors would like to thank the Wadsworth Center Tissue Culture Core facility for providing cells and media. We thank Aaron Shatkin at Rutgers, the State University of New Jersey for providing us the plasmid for expression of recombinant human guanine N-7 RNA methyltransferase.

References

Assenberg, R., Ren, J., Verma, A., Walter, T.S., Alderton, D., Hurrelbrink, R.J., Fuller, S.D., Bressanelli, S., Owens, R.J., Stuart, D.I., Grimes, J.M., 2007. Crystal structure of the Murray Valley encephalitis virus NS5 methyltransferase domain in complex with cap analogues. J. Gen. Virol. 88, 2228–2236.

Benarroch, D., Egloff, M.P., Mulard, L., Guerreiro, C., Romette, J.L., Canard, B., 2004. A structural basis for the inhibition of the NS5 dengue virus mRNA 2′-O-methyltransferase domain by ribavirin 5′-triphosphate. J. Biol. Chem. 279, 35638–35643.

Bhattacharya, D., Hoover, S., Falk, S.P., Weisblum, B., Vestling, M., Striker, R., 2008. Phosphorylation of yellow fever virus NS5 alters methyltransferase activity. Virology 380, 276–284.

Brooks, B.R., Brooks 3rd, C.L., Mackerell Jr., A.D., Nilsson, L., Petrella, R.J., Roux, B., Won, Y., Archontis, G., Bartels, C., Boresch, S., Caflisch, A., Caves, L., Cui, Q., Dinner, A.R., Feig, M., Fischer, S., Gao, J., Hodoscek, M., Im, W., Kuczera, K., Lazaridis, T., Ma, J., Ovchinnikov, V., Paci, E., Pastor, R.W., Post, C.B., Pu, J.Z., Schaefer, M., Tidor, B., Venable, R.M., Woodcock, H.L., Wu, X., Yang, W., York, D.M., Karplus, M., 2009. CHARMM: the biomolecular simulation program. J. Comput. Chem. 30, 1545–1614.

Burke, D.S., Monath, T.P., 2001. Flaviviruses, Fourth ed. Lippincott William & Wilkins.

CDC, 2010. CDC West Nile virus homepage. <http://www.cdc.gov/ncidod/dvbid/westnile/surv&controlCaseCount03.htm>.

Cheng, Y., Prusoff, W.H., 1973. Relationship between the inhibition constant (K1) and the concentration of inhibitor which causes 50 per cent inhibition (I50) of an enzymatic reaction. Biochem. Pharmacol. 22, 3099–3108.

Chung, K.Y., Dong, H., Chao, A.T., Shi, P.Y., Lescar, J., Lim, S.P., 2010. Higher catalytic efficiency of N-7-methylation is responsible for processive N-7 and 2′-O methyltransferase activity in dengue virus. Virology 402, 52–60.

Copeland, R.A., 2005. Lead optimization and structure-activity relationships for reversible inhibitors. In: Copeland, R.A. (Ed.), Evaluation of Enzyme Inhibitors in Drug Discovery: A Guide for Medicinal Chemists and Pharmacologists, fitrst ed. John Wiley & Sons, Inc., Hoboken, New Jersey.

Dong, H., Ray, D., Ren, S., Zhang, B., Puig-Basagoiti, F., Takagi, Y., Ho, C.K., Li, H., Shi, P.Y., 2007. Distinct RNA elements confer specificity to flavivirus RNA cap methylation events. J. Virol. 81, 4412–4421.

Dong, H., Ren, S., Li, H., Shi, P.Y., 2008a. Separate molecules of West Nile virus methyltransferase can independently catalyze the N7 and 2′-O methylations of viral RNA cap. Virology 377, 1–6.

Dong, H., Ren, S., Zhang, B., Zhou, Y., Puig-Basagoiti, F., Li, H., Shi, P.Y., 2008b. West Nile virus methyltransferase catalyzes two methylations of the viral RNA cap through a substrate-repositioning mechanism. J. Virol. 82, 4295–4307.

Dong, H., Liu, L., Zou, G., Zhao, Y., Li, Z., Lim, S.P., Shi, P.Y., Li, H., 2010. Structural and functional analyses of a conserved hydrophobic pocket of flavivirus methyltransferase. J. Biol. Chem. 285, 32586–32595.

Egloff, M.P., Benarroch, D., Selisko, B., Romette, J.L., Canard, B., 2002. An RNA cap (nucleoside-2′-O-)-methyltransferase in the flavivirus RNA polymerase NS5: crystal structure and functional characterization. EMBO J. 21, 2757–2768.

Egloff, M.P., Decroly, E., Malet, H., Selisko, B., Benarroch, D., Ferron, F., Canard, B., 2007. Structural and functional analysis of methylation and 5′-RNA sequence requirements of short capped RNAs by the methyltransferase domain of dengue virus NS5. J. Mol. Biol. 372, 723–736.

Furuichi, Y., Shatkin, A.J., 2000. Viral and cellular mRNA capping: past and prospects. Adv. Virus Res. 55, 135–184.

Geiss, B.J., Thompson, A.A., Andrews, A.J., Sons, R.L., Gari, H.H., Keenan, S.M., Peersen, O.B., 2009. Analysis of flavivirus NS5 methyltransferase cap binding. J. Mol. Biol. 385, 1643–1654.

Ghosh, A.K., Kass, J., 2010. Highly diastereoselective synthesis of modified nucleosides via an asymmetric multicomponent reaction. Chem. Commun. (Camb.) 46, 1218–1220.

Khromykh, A.A., Kenney, M.T., Westaway, E.G., 1998. Trans-complementation of flavivirus RNA polymerase gene NS5 by using Kunjin virus replicon-expressing BHK cells. J. Virol. 72, 7270–7279.

Kramer, L.D., Li, J., Shi, P.Y., 2007. West Nile virus. Lancet Neurol. 6, 171–181.

Kroschewski, H., Lim, S.P., Butcher, R.E., Yap, T.L., Lescar, J., Wright, P.J., Vasudevan, S.G., Davidson, A.D., 2008. Mutagenesis of the dengue virus type 2 NS5 methyltransferase domain. J. Biol. Chem. 283, 19410–19421.

Lim, S.P., Wen, D., Yap, T.L., Yan, C.K., Lescar, J., Vasudevan, S.G., 2008. A scintillation proximity assay for dengue virus NS5 2′-O-methyltransferase-kinetic and inhibition analyses. Antiviral Res. 80, 360–369.

Lim, S.P., Sonntag, L.S., Noble, C., Nilar, S.H., Ng, R.H., Zou, G., Monaghan, P., Chung, K.Y., Dong, H., Liu, B., Bodenreider, C., Lee, G., Ding, M., Chan, W.L., Wang, G., Jian, Y.L., Chao, A.T., Lescar, J., Yin, Z., Vedananda, T.R., Keller, T.H., Shi, P.Y., 2011. Small molecule inhibitors that selectively block dengue virus methyltransferase. J. Biol. Chem. 286, 6233–6240.

Liu, L., Dong, H., Chen, H., Zhang, J., Ling, H., Li, Z., Shi, P.Y., Li, H., 2010. Flavivirus RNA cap methyltransferase: structure, function, and inhibition. Front. Biol. 5, 286–303.

Longley, D.B., Harkin, D.P., Johnston, P.G., 2003. 5-Fluorouracil: mechanisms of action and clinical strategies. Nat. Rev. Cancer 3, 330–338.

Luzhkov, V.B., Selisko, B., Nordqvist, A., Peyrane, F., Decroly, E., Alvarez, K., Karlen, A., Canard, B., Qvist, J., 2007. Virtual screening and bioassay study of novel inhibitors for dengue virus mRNA cap (nucleoside-2′O)-methyltransferase. Bioorg. Med. Chem. 15, 7795–7802.

Malde, A.K., Zuo, L., Breeze, M., Stroet, M., Poger, D., Nair, P.C., Oostenbrink, C., Mark, A.E., 2011. An automated force field topology builder (ATB) and repository: version 1.0. J. Chem. Theory Comput. 7, 4026–4037.

Milani, M., Mastrangelo, E., Bollati, M., Selisko, B., Decroly, E., Bouvet, M., Canard, B., Bolognesi, M., 2009. Flaviviral methyltransferase/RNA interaction: structural basis for enzyme inhibition. Antiviral Res. 83, 28–34.

Miteva, M.A., Guyon, F., Tuffery, P., 2010. Frog2: efficient 3D conformation ensemble generator for small compounds. Nucleic Acids Res. 38, W622–627.

Pillutla, R.C., Yue, Z., Maldonado, E., Shatkin, A.J., 1998. Recombinant human mRNA cap methyltransferase binds capping enzyme/RNA polymerase IIo complexes. J. Biol. Chem. 273, 21443–21446.

Podvinec, M., Lim, S.P., Schmidt, T., Scarsi, M., Wen, D., Sonntag, L.S., Sanschagrin, P., Shenkin, P.S., Schwede, T., 2010. Novel inhibitors of dengue virus methyltransferase: discovery by in vitro-driven virtual screening on a desktop computer grid. J. Med. Chem. 53, 1483–1495.

Prinz, H., 2010. Hill coefficients, dose-response curves and allosteric mechanisms. J. Chem. Biol. 3, 37–44.

Ray, D., Shah, A., Tilgner, M., Guo, Y., Zhao, Y., Dong, H., Deas, T.S., Zhou, Y., Li, H., Shi, P.Y., 2006. West Nile virus 5′-cap structure is formed by sequential guanine N-7 and ribose 2′-O methylations by nonstructural protein 5. J. Virol. 80, 8362–8370.

Sampath, A., Padmanabhan, R., 2009. Molecular targets for flavivirus drug discovery. Antiviral Res. 81, 6–15.

Selisko, B., Peyrane, F.F., Canard, B., Alvarez, K., Decroly, E., 2010. Biochemical characterization of the (nucleoside-2′O)-methyltransferase activity of dengue virus protein NS5 using purified capped RNA oligonucleotides (7Me)GpppAC(n) and GpppAC(n). J. Gen. Virol. 91, 112–121.

Shoichet, B.K., 2006. Interpreting steep dose–response curves in early inhibitor discovery. J. Med. Chem. 49, 7274–7277.

USGS, 2010. Disease Maps 2010. <http://diseasemaps.usgs.gov/>.

Vanommeslaeghe, K., Hatcher, E., Acharya, C., Kundu, S., Zhong, S., Shim, J., Darian, E., Guvench, O., Lopes, P., Vorobyov, I., Mackerell Jr., A.D., 2010. CHARMM general force field: a force field for drug-like molecules compatible with the CHARMM all-atom additive biological force fields. J. Comput. Chem. 31, 671–690.

Yap, L.J., Luo, D., Chung, K.Y., Lim, S.P., Bodenreider, C., Noble, C., Shi, P.Y., Lescar, J., 2010. Crystal structure of the dengue virus methyltransferase bound to a 5′-capped octameric RNA. PLoS ONE 5.

Zhou, Y., Ray, D., Zhao, Y., Dong, H., Ren, S., Li, Z., Guo, Y., Bernard, K.A., Shi, P.Y., Li, H., 2007. Structure and function of flavivirus NS5 methyltransferase. J. Virol. 81, 3891–3903.